



Linear and nonlinear optical properties change in Ag/GeS heterostructure thin films by thermal annealing and laser irradiation

R. Naik¹ · A. Aparimita² · D. Alagarasan³ · S. Varadharajaperumal⁴ · R. Ganesan³

Received: 3 October 2019 / Accepted: 1 February 2020 / Published online: 17 February 2020
© Springer Science+Business Media, LLC, part of Springer Nature 2020

Abstract

The photo and thermal annealing induced linear and nonlinear optical properties, structural properties and surface morphology of thermally evaporated Ag/GeS bilayer thin films are reported in the present study. The related changes due to Ag diffusion into GeS layer by annealing at 200 °C and 532 nm laser irradiation have been probed. The X-ray diffraction revealed no structural change whereas the surface structure was viewed by field emission scanning electron microscopy. The optical data recorded by UV–visible spectrophotometer in the range of 500–1200 nm shows the decrease in refractive index (n) and extinction coefficient (k). The Ag diffusion into GeS layer increased the optical band gap due to the decrease of width of the localised states. The single oscillator Wemple–Di Domenico model was used to study the dispersion relation. The third order nonlinear susceptibility ($\chi^{(3)}$) and nonlinear refractive index (n_2) were calculated by using suitable semi-empirical relation. The change in density of defects and localised states explained the observed linear and nonlinear changes with annealing and laser irradiation. The homopolar bond to heteropolar bond transformation is noticed from X-ray photoelectron spectroscopy. The observed optical changes can be used in various optical applications.

Keywords Thin films · Annealing · Optical properties · Laser irradiation · Refractive index · Nonlinear properties

✉ R. Naik
ramakanta.naik@gmail.com

¹ Department of Engineering and Material Physics, Institute of Chemical Technology-Indian Oil Odisha Campus, Bhubaneswar 751013, India

² Department of Physics, Utkal University, Bhubaneswar 751004, India

³ Department of Physics, Indian Institute of Science, Bangalore 560012, India

⁴ Centre for Nano Science and Engineering, Indian Institute of Science, Bangalore 560012, India

1 Introduction

The amorphous chalcogenide alloys consist of one chalcogen element (S, Se Te) as a major constituent and other electropositive elements. These materials possess semiconducting behaviour along with high IR transmitting power (Calvez 2017). Their low phonon energy and low non-radiative decay rates found in large scale IR applications (Galstyan et al. 2015). The other important applications include active and passive solid-state electronics, opto-electronic devices, optical switching and optical signal processing due to their high IR transmittance and high third order optical nonlinearity (Ying et al. 2015; Rashad et al. 2018; Plesa et al. 2015; Fang et al. 2018). In this regard, the Ge–S alloys were widely used in photonic applications and optical devices (Shoulders et al. 2013; Rana et al. 2018; Kohoutek et al. 2011). However, the 3rd order nonlinearity was enhanced by the doping of Ag atoms into such alloys for suitable nonlinear applications (Kolobov and Elliott 1991). The degree of change by Ag addition depends on the method of doping. In this respect, thermal annealing and laser irradiation are two prominent techniques for incorporation of third element into the host matrix. Some of the results include the light induced diffusion of Ag into Ge₃₀S₇₀ that creates low relief resist masks used in diffractive optics (Eneva et al. 1999). The Ar laser treatment on Ag/As₃₀S₇₀ film is used to fabricate holographic phase gratings (Wagner et al. 2003) and waveguides were made from the Ag/GeS₂ bilayer by UV laser micromanipulation (Kanai et al. 2010). The availability of lone pair p-states and flexible nature of chalcogenides are the root cause of photoinduced phenomena (Zakery and Elliott 2003). The changes occurring at diffusion site and its surrounding are equally important for application purpose (Murakami et al. 2015). The magnitude of changes by photo diffusion of Ag in bilayer film is comparatively more than that of bulk form (Kawaguchi and Maruno 1992). The Ag doping into GeS₂ film increased the data retention capacity in CBRAM devices (Longnos et al. 2013). The formation of harmonic and an-harmonic phonons by photo induced effects in chalcogenide films is useful for nonlinear optics (Xue et al. 2012; Shpotyuk et al. 1997).

Likewise, thermal annealing is also regarded as one of the simple methods to stimulate the various properties of chalcogenide thin films. The thermal diffused refractive index change in Ag/As₂Se₃ bilayer film is relatively more than that of photoinduced one (Aparimita et al. 2018a). Both photodarkening and photobleaching effects have been noticed in Sb doped As–S film on annealing and irradiation (Naik et al. 2011). The solar cell absorbing material is being formed by thermal annealing induced Ag diffusion into Ag/In/Ag/In layer (Panda et al. 2018). The optical and structural properties of metal/chalcogenide heterostructure film changes with photo and thermal annealing (Horton et al. 1996; Behera et al. 2017). In respect to the important findings as discussed above, the nonlinear optical properties change by both photo and thermal annealing in Ag/GeS heterostructure films is not investigated which drives us for the present study.

In our present investigation, we have observed the extent of change in the linear and nonlinear optical constants due to Ag diffusion into GeS layer. The linear optical parameters such as refractive index, optical band gap, absorption coefficient, dispersion energy, oscillator energy, dielectric constants, Urbach energy of the studied films have been evaluated from the transmission data recorded by UV–visible spectrometer. The dispersion of refractive index was calculated and discussed on the basis of single oscillator model. The nonlinear susceptibility (χ^3) and nonlinear refractive index (n_2) were calculated from the linear refractive index using Miller's rule. The chemical bond redistribution due to photo-thermal process was probed by X-ray photo electron spectroscopy (XPS). The structure

of the films was probed by X-ray diffraction (XRD) and the surface morphology by field emission scanning electron microscopy (FESEM).

2 Experimental procedure

The Ag/GeS heterostructure films (Ag ~ 10 nm and GeS ~ 800 nm) were prepared by thermal evaporation method (Hind Hivac 12A4D coating unit) at a vacuum of $\sim 10^{-5}$ Torr. The deposition rate was ~ 2 nm/s which was displayed in the quartz crystal monitor attached with the coating unit. The substrate holder rotated continuously to obtain a homogenous and uniform film. The as-prepared Ag/GeS film was annealed at 200 °C for 2 h and another as-prepared Ag/GeS film was irradiated for 2 h by 532 nm CW laser with intensity of 4 mW cm⁻². The laser exposed area was ~ 3 mm in radius on the film which was mounted on a sample holder. We have calculated the temperature developed at the illuminated region due to laser irradiation by the procedure followed in Ganjoo et al. (2000) which comes ~ 7 K. This infers the observed changes are due to incident photon energy from the laser light and developed heat is not inducing any thermal change as this small temperature rise is not enough to induce any change as reported in other studies (Naik et al. 2009a; Ganjoo and Jain 2006).

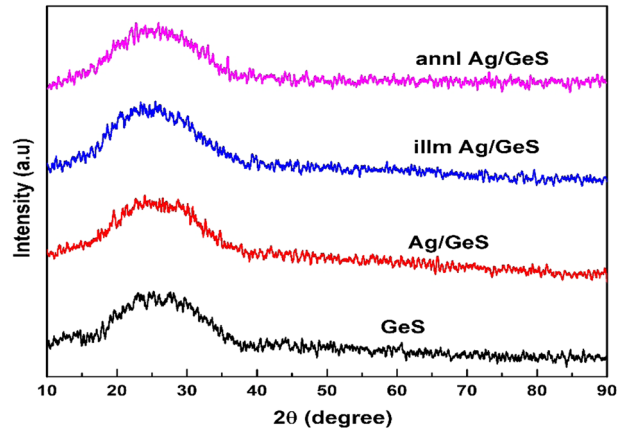
The XRD was done with Cu-K α radiation (Bruker D8 Advance, $\lambda = 1.54$ Å) at 40 kV voltage with 40 mA current. The scanning was done in the 2θ range between 10° and 90°. The presence of different elements after deposition in both as-prepared GeS and Ag/GeS thin film was verified by Energy dispersive X-ray analysis (EDX) with an attachment of FESEM facility (ZEISS SIGMA-40). The FESEM images on 1 cm² size sample were taken at $\sim 2 \times 10^{-7}$ Torr pressure. The optical transmittance spectra between 500 and 1200 nm were taken by UV-visible spectrometer (Bruker Optics, IFS66v/S) at dark condition inside the sample chamber. The linear optical quantities like absorption coefficient (α), optical band gap (E_g), and Tauc parameter ($B^{1/2}$) were calculated from Tauc relation whereas Swanepoel method was used to calculate linear refractive index. The dispersion parameters were obtained from single oscillator Wemple–Di Domenico model. The nonlinear refractive index (n_2), 3rd order susceptibility (χ^3) was evaluated by Miller's formula. The chemical bonding modifications induced by Ag diffusion by photo and thermal annealing was measured in XPS (Axis Ultra, Kratos Analytical, UK) to support the optical changes. The required XPS core level spectra were taken with Al K α X-rays (1486.6 eV) at a base vacuum of 2×10^{-9} Torr. Due to the insulating nature of these glassy materials, the charge correction was done by taking the adventitious C1s line binding energy (BE) as 284.6 eV (Barr and Seal 1995; Naik et al. 2009b). The original BE data were corrected according to the calculated calibration factor. The measurement was performed on different portion of the films to reproduce the exact data.

3 Result and discussion

3.1 Structural and surface morphology study

The XRD pattern of the as-deposited GeS, Ag/GeS, irradiated and annealed Ag/GeS thin films is shown in Fig. 1. The obtained pattern indicates the absence of any sharp peaks inferring the amorphous nature of the as-prepared GeS and Ag/GeS film. The

Fig. 1 XRD pattern of GeS, Ag/GeS, illuminated and annealed Ag/GeS thin films



amorphous nature sustains after both thermal and photo induced phenomena as seen from Fig. 1. The broad hump from 15° to 35° signifies the amorphous nature of the studied films. So, there is no structural transformation occurring in the annealed and irradiated film. However, the Ag diffusion in Se brings the new phase Ag_2Se as reported in our earlier study which is not seen in the present case of Ag/GeS film (Naik et al. 2019a).

The presence of Ge, S in the as-prepared GeS and the presence of Ge, S, Ag in Ag/GeS thin film was confirmed by EDX analysis as shown in Fig. 2a, b respectively. The peak intensity of Ag is very low as compared to that of Ge and S because of very thin Ag layer (10 nm) deposition on bottom GeS layer. The composition of the films is given in the Table 1.

Figure 3a–d show the FESEM images of as deposited GeS, Ag/GeS, illuminated and annealed Ag/GeS heterostructure films respectively. The picture reveals the uniformity and smoothness of the studied films. As all the films are similar in nature which infers that there is no structural change as seen from XRD. The images do not show any growth of the particles which also confirms the amorphous nature of thin films.

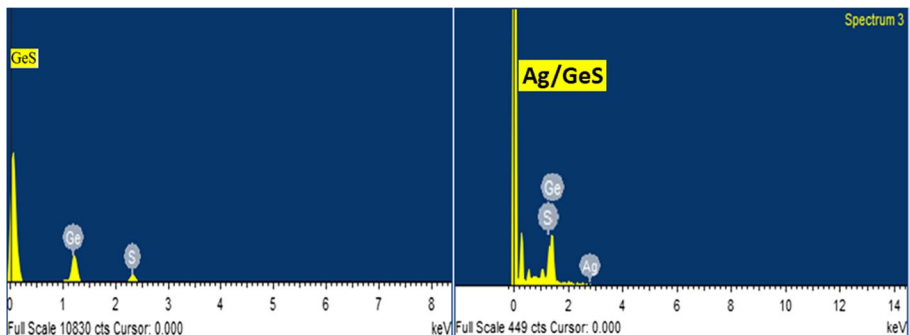
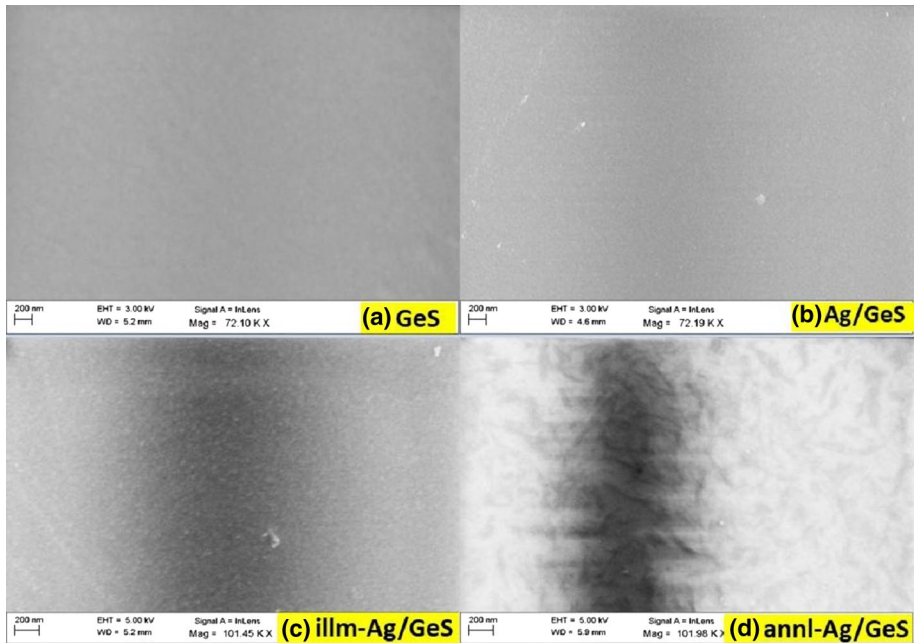


Fig. 2 EDX spectra of **a** GeS and **b** Ag/GeS bilayer thin film

Table 1 EDX data for the different elements in GeS and Ag/GeS thin films

| Element | GeS | | Ag/GeS | |
|---------|-----------|------------|-----------|------------|
| | M. Weight | Atomic wt% | M. Weight | Atomic wt% |
| Ge | 75.83 | 58.08 | 70.04 | 50.53 |
| S | 24.17 | 41.92 | 21.91 | 38.39 |
| Ag | 0 | 0 | 08.05 | 11.08 |
| Total | 100 | 100 | 100 | 100 |

**Fig. 3** FESEM images of **a** GeS, **b** Ag/GeS, **c** illuminated Ag/GeS and **d** annealed Ag/GeS thin films

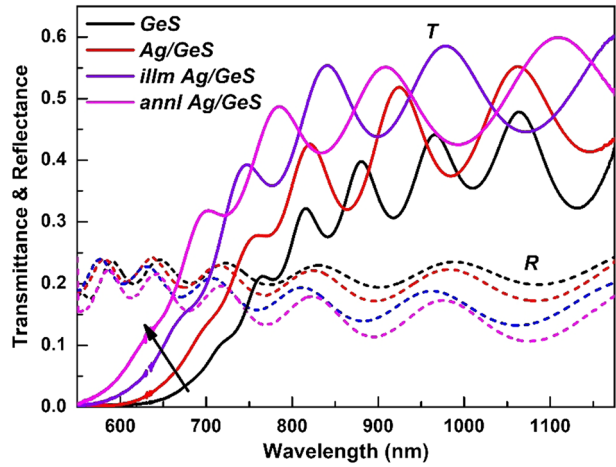
3.2 Linear optical parameters

3.2.1 Transmission, absorption and extinction coefficient

The optical transmittance data plotted in Fig. 4 shows the presence of several interference fringes that represent the uniformity and homogeneity of the prepared films (Shaaban et al. 2013; Naik et al. 2016). The transmission was 28% at 800 nm for GeS film where as it increased to 37% with Ag deposition onto GeS layer (Ag/GeS film). After laser irradiation and annealing, its value further increased to 43% and 47% respectively for the Ag/GeS thin film. Such amount of increase in transmission % is a clear indication of Ag diffusion into bottom GeS layer. However, the extent of change is different for thermal and laser induced cases.

The annealing and irradiation also bring changes in absorption edge that shows a shift towards lower wavelength (higher energy). The absorption power called as coefficient

Fig. 4 Transmittance and Reflectance spectra of GeS, Ag/GeS, illuminated and annealed Ag/GeS thin films

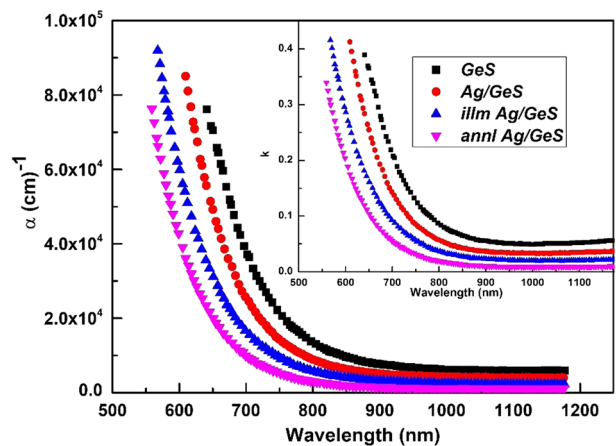


(α) of the investigated films was calculated from the transmittance and reflectance data using the relation (Shaaban et al. 2013; Valalova et al. 2000)

$$\alpha = \frac{1}{d} \ln \left[\frac{(1 - R)^2 + [(1 - R)^4 + 4R^2T^2]^{1/2}}{2T} \right] \tag{1}$$

where d , R and T are the thickness of the film, reflectance and transmittance respectively. The evaluated α values as a function of wavelength (λ) for the as-prepared, thermally annealed and irradiated films are shown in Fig. 5. The strong absorption region lies in the wavelength range 550–700 nm that was found to be reduced with λ for the annealed and irradiated film. The decrease in α value for the annealed and irradiated films is the consequence of increase in transmittance and decrease in density of defect states which enhanced the optical band gap.

Fig. 5 α versus λ plot (inset k vs. λ) of GeS, Ag/GeS, illuminated and annealed Ag/GeS thin films



The mass extinction coefficient (k) that measures how strongly the film absorbs the light at given λ is related with the absorption coefficient and wavelength by (Naik et al. 2019b).

$$k = \frac{\alpha\lambda}{4\pi} \tag{2}$$

The variation of k with λ is shown in Fig. 5 (inset) that depicts the decrease in k value with both the energy treatments. Since k is related to the surface defects and disorder caused by the diffusion of Ag into GeS layer, it infers the decrease in density of defect states leading to the increase in E_g .

3.2.2 Optical band gap (E_g), Tauc parameter ($B^{1/2}$) and Urbach energy (E_u)

The optical band gap of the studied films were calculated at the high absorption region corresponding to the transitions between extended states in valence and conduction band from Tauc relation (Tauc 1979) as given by

$$ah\nu = B(h\nu - E_g)^n \tag{3}$$

where $h\nu$ is the photon energy and B is a constant called as Tauc parameter that gives electronic transition probability and degree of disorder present in the film. The power factor n in Eq. 3 has different values for different type of transitions such as $n=1/2, 3/2, 2$ and 3 for direct allowed, direct forbidden indirect allowed and indirect forbidden transition respectively (Naik and Ganesan 2015). The present data fits best with $n=2$ which shows the indirect allowed type transition. The x-intercept of the straight-line fitting for linear portion of $(ah\nu)^{1/2}$ versus $h\nu$ for the films which gives optical band gap (E_g) is shown in Fig. 6. The obtained values are presented in Table 2 that shows the E_g value increased from 1.41 ± 0.02 eV (GeS) to 1.47 ± 0.01 eV (Ag/GeS) after Ag addition onto GeS matrix. The band gap increased to 1.58 ± 0.02 eV for laser irradiated film and 1.65 ± 0.01 eV for the annealed film. An increment of 0.18 eV in E_g for the annealed film is more than that of 0.11 eV change for the irradiated film. This is an evidence of strongness of thermal annealing induced effect over laser irradiation.

Fig. 6 $(ah\nu)^{1/2}$ versus $h\nu$ for GeS, Ag/GeS, illuminated and annealed Ag/GeS thin films

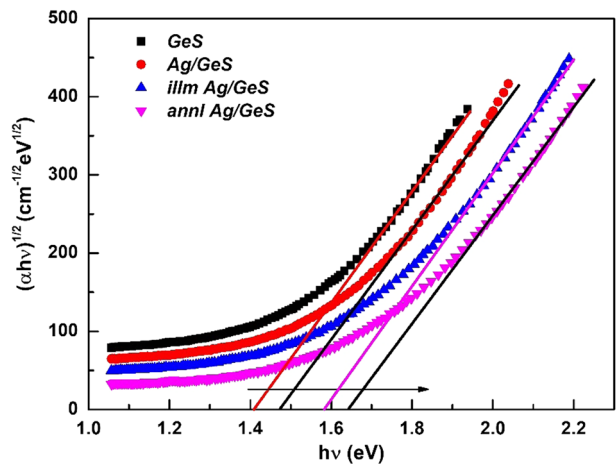


Table 2 The optical parameters of the studied films

| Sample | E_g (eV) | $B^{1/2}$ ($\text{cm}^{-1/2} \text{eV}^{-1/2}$) | E_u (meV) | E_0 (eV) | E_d (eV) | n_0 | ϵ_∞ | ϵ_L | $N/m^* \times 10^{17}$ ($\text{cm}^{-3} \text{eV}^{-1}$) |
|-------------|-----------------|--|-------------|------------|------------|-------|-------------------|--------------|---|
| GeS | 1.41 ± 0.02 | 772 ± 1 | 211 ± 1 | 2.55 | 13.33 | 2.495 | 6.225 | 10.53 | 2.53 |
| Ag/GeS | 1.47 ± 0.01 | 783 ± 2 | 197 ± 2 | 2.57 | 13.37 | 2.49 | 6.2 | 9.88 | 2.48 |
| illm-Ag/GeS | 1.58 ± 0.02 | 802 ± 2 | 176 ± 2 | 3.58 | 16.56 | 2.385 | 5.688 | 7.64 | 1.28 |
| annl-Ag/GeS | 1.65 ± 0.02 | 824 ± 1 | 154 ± 3 | 3.67 | 16.64 | 2.352 | 5.531 | 7.24 | 1.22 |

The increase in E_g after heat treatment and light exposure is well understood by Mott and Davis model (Mott and Davis 1979) which proposes that the number of defects and degree of disorder influences the width of the localized states near the mobility edge in amorphous structure. The localized states have a strong influence on the optical absorption and thus on the optical band gap. The heat and photon energy annealed out the defect states by Ag atoms diffusion into the GeS layer that converts wrong homopolar bonds to a greater number of heteropolar Ag–S bonds. This process reduces the degree of disorder in the annealed and irradiated films. Therefore, the magnitude of density of defects decreased which reduces the width of the localized states and consequently, the E_g value increased for the annealed and irradiated film (El-Nahass et al. 2014; Panda et al. 2019).

The measure of disorder is represented by Tauc parameter ($B^{1/2}$) which is found as the slope of the fitting in Eq. 3 (Zanatta and Chambouleyron 1996). The value of $B^{1/2}$ for GeS film is $772 \pm 1 \text{ cm}^{-1/2} \text{ eV}^{-1/2}$ which then increased to $783 \pm 2 \text{ cm}^{-1/2} \text{ eV}^{-1/2}$ for Ag/GeS. After light exposure and thermal annealing, the value raised to $802 \pm 2 \text{ cm}^{-1/2} \text{ eV}^{-1/2}$ and $824 \pm 1 \text{ cm}^{-1/2} \text{ eV}^{-1/2}$ respectively. From the values, it is understood that the disorder decreased after thermal annealing and laser irradiation as predicted in Mott Davis Model.

The tail width of the localized states E_u (Urbach energy) also measures amount of disorder in a system. This parameter is being evaluated in the weak absorption region of the absorption spectrum from an exponential dependence on photon energy (Urbach 1953)

$$\alpha(h\nu) = \alpha_0 \exp\left(\frac{h\nu}{E_u}\right) \quad (4)$$

where ν is the frequency of the radiation, α_0 is a constant, h is Planck's constant. The E_u was evaluated from the reciprocal of the slope of the linear portion of the dependence of $\ln(\alpha/\alpha_0)$ versus $h\nu$. The calculated E_u values for the as-deposited GeS and Ag/GeS thin films are $211 \pm 1 \text{ meV}$ and $197 \pm 2 \text{ meV}$ respectively which further reduced to $176 \pm 2 \text{ meV}$ for irradiated and $154 \pm 3 \text{ meV}$ for annealed film. The reduced E_u values confirm the decrease of disorder in the photo and thermally annealed films. The presented values of $B^{1/2}$ and E_u shows the inverse relation between them as studied in various films (Atyia and Hageb 2016; Pradhan et al. 2017).

3.2.3 Linear refractive Index (n), oscillator energy (E_0), dispersion energy (E_d)

By applying Swanepoel method (Swanepoel 1983), in the transparent region where the absorption coefficient $\alpha \rightarrow 0$, the n value is calculated by

$$n = \left[N + (N^2 - s^2)^{1/2} \right]^{1/2} \tag{5}$$

where $N = 2s \frac{T_M - T_m}{T_M T_m} + \frac{S^2 + 1}{2}$

where T_M refers to the transmission at maxima and T_m refers to the transmission at minima point corresponding to a particular λ and s is the refractive index of glass substrate (1.51). The refractive index of the as-prepared Ag/GeS film decreased from GeS film. The n value decreased upon annealing and irradiation as shown in Fig. 7. The variation of band gap and refractive index is related by Moss rule which states that $E_g n^4 \approx \text{constant}$ (Attia et al. 2013). So, the change in the band gap (red shift/blue shift in the absorption edge) is related to a change in the refractive index (Aparimita et al. 2018b).

The dispersion of refractive index in the films upon photo and thermal annealing plays an important role in various photonic applications. The single effective oscillator formula developed by Wemple–DiDomenico (1971) evaluates the dispersion parameter which is given by

$$n^2 - 1 = \frac{E_d E_0}{E_0^2 - hv^2} \tag{6}$$

where E_0 and E_d are effective oscillator energy and dispersion energy respectively. The dispersion energy measures the average strength of inter band optical transitions (Shaaban et al. 2018). The two values were determined from the plot $(n^2 - 1)^{-1}$ against $(hv)^2$ as shown in Fig. 8. The $\frac{E_0}{E_d}$ represents the intercept on the vertical axis and $(E_0 E_d)^{-1}$ is the slope of the fitting from which E_0 and E_d were evaluated.

The static refractive index (n_0) is determined by the formula

$$n_0^2 - 1 = \frac{E_0}{E_d} \tag{7}$$

Fig. 7 n versus λ plot of GeS, Ag/GeS, illuminated and annealed Ag/GeS thin films

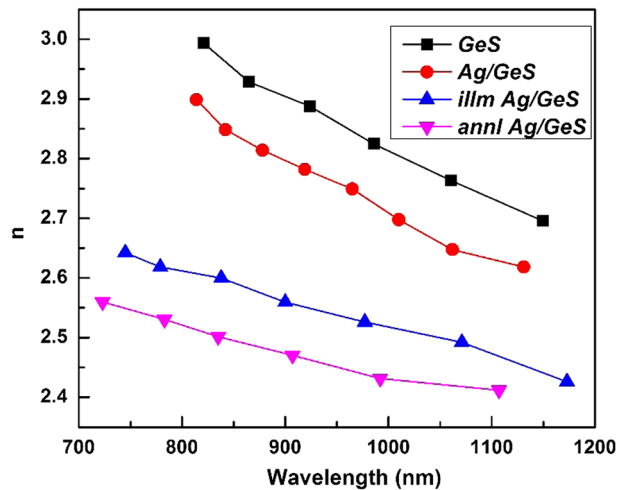
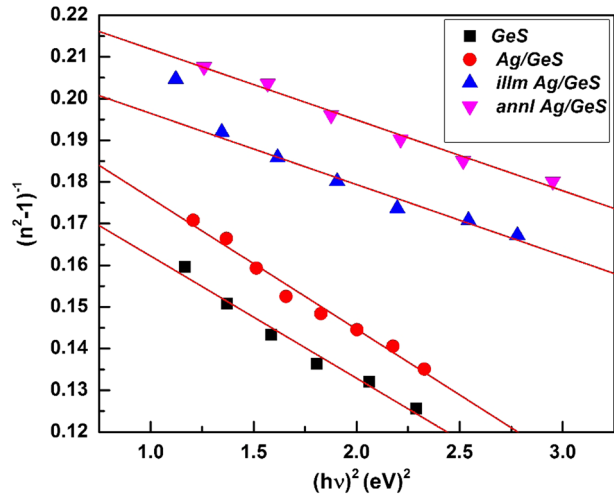


Fig. 8 $(n^2 - 1)^{-1}$ versus $(h\nu)^2$ plot of GeS, Ag/GeS, illuminated and annealed Ag/GeS thin films



The high frequency dielectric constant $\epsilon_\infty = n_0^2$ is being calculated and presented in Table 2. From the data values presented in Table 2, it is observed that E_0 and E_d values increased with annealing and irradiation process. The decreasing nature of high frequency dielectric constant ϵ_∞ after Ag deposition and diffusion into GeS film is good for optical communication.

3.2.4 High frequency dielectric constant and carrier concentration

The high frequency dielectric constant (ϵ_L) is being calculated from the linear refractive index by the relation (Edward 1985)

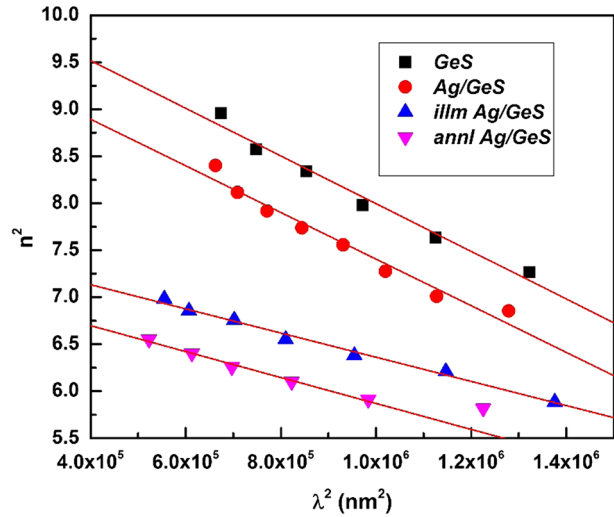
$$n^2 = \epsilon_L - \left(\frac{e^2 N}{4\pi^2 C^2 \epsilon_0 m^*} \right) \lambda^2 \tag{8}$$

where e , N , ϵ_0 , m^* , c is the charge of electron, free charge carrier concentration, permittivity of free space, effective mass of charge carrier and velocity of light respectively. The Fig. 9 shows the change in n^2 with λ^2 in which the straight-line fitting gives the ϵ_L as intercept and N/m^* as slope. The obtained ϵ_L and N/m^* values for all the films are listed in Table 2. The $\epsilon_L > \epsilon_\infty$ nature is due to the increase in free charge carrier concentration in the film (El-Nahass et al. 2008, 2014).

3.3 Nonlinear optical susceptibility and nonlinear refractive index

The nonlinear optical quantities are internally connected with the nonlinear polarization and the incident energy. Since amorphous materials possess high nonlinear optical susceptibility, nonlinear optical elements and optical switching devices are fabricated from them (Sharma et al. 2014). The third order harmonic generation, two-photon absorption and nonlinear refractive index are evaluated from the third order nonlinear optical susceptibility $\chi^{(3)}$ for nonlinear optical applications (Abuelwafa et al. 2015). The linear susceptibility $\chi^{(1)}$ and nonlinear susceptibility $\chi^{(3)}$ are related by Miller’s formula (Wayne 1969)

Fig. 9 n^2 versus λ^2 plot of GeS, Ag/GeS, illuminated and annealed Ag/GeS thin films



$$\chi^{(3)} \cong A (\chi^{(1)})^4 \tag{9}$$

where $A = 1.7 \times 10^{-10}$ (χ measured in esu).

The linear susceptibility is given by $\chi^{(1)} = (n^2 - 1)/4\pi$ which in long wavelength limit ($h\nu \rightarrow 0$) turns down to $\chi^{(1)} = (n_0^2 - 1)/4\pi$. So, the Eq. 9 can be written as

$$\chi^{(3)} \cong A (n_0^2 - 1)^4 / (4\pi)^4 \tag{10}$$

By putting the value of n_0^2 (Eq. 7), we can rewrite Eq. 10 as

$$\chi^{(3)} = A \left[\frac{E_d}{4\pi E_0} \right]^4 \tag{11}$$

The value of nonlinear refractive index n_2 is deduced from $\chi^{(3)}$ by the formula

$$n_2 = \frac{12\pi\chi^{(3)}}{n_0} \tag{12}$$

The obtained values of $\chi^{(1)}$, $\chi^{(3)}$, n_2 are presented in Table 3 from which we can notice that $\chi^{(3)}$ value decreased after thermal annealing and laser irradiation. The monotonic decrease of susceptibility with increasing band gap is shown in Fig. 10 which is also reported in other studies (El-Nahass et al. 2008, 2014). The decrease of E_d/E_0 ratio results

Table 3 Optical parameters derived from the transmission spectra for GeS and Ag/GeS thin films

| Sample | $\chi^{(1)} (h\nu \rightarrow 0)$ | $\chi^{(3)} (h\nu \rightarrow 0)$ ($\times 10^{-12}$ esu) | $n_2 (\times 10^{-10}$ esu) |
|-------------|-----------------------------------|---|-----------------------------|
| GeS | 0.416 ± 0.001 | 5.1 ± 0.01 | 0.77 ± 0.01 |
| Ag/GeS | 0.414 ± 0.001 | 5.0 ± 0.01 | 0.75 ± 0.01 |
| illm-Ag/GeS | 0.368 ± 0.002 | 3.1 ± 0.01 | 0.49 ± 0.01 |
| annl-Ag/GeS | 0.361 ± 0.001 | 2.8 ± 0.02 | 0.46 ± 0.01 |

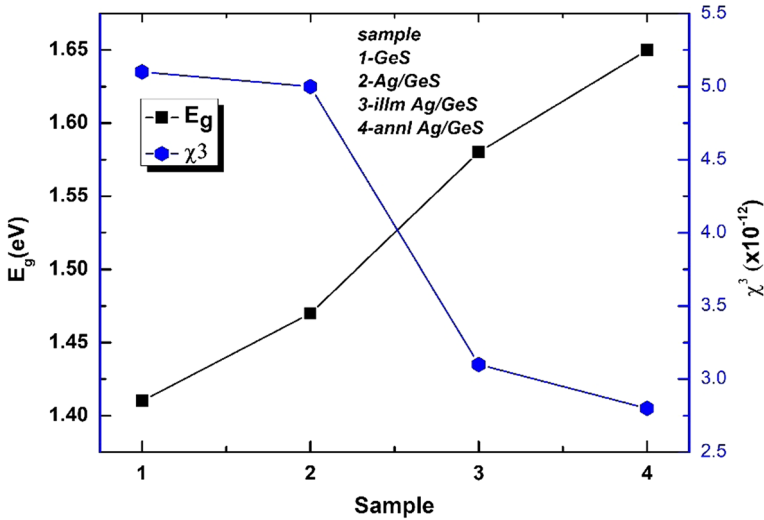


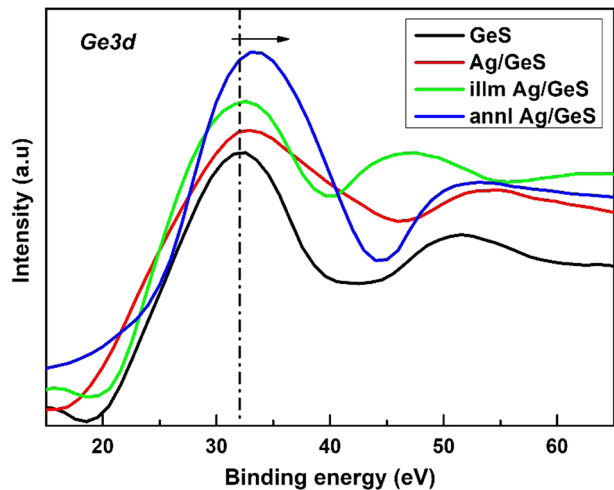
Fig. 10 E_g versus $\chi^{(3)}$ plot for different studied samples

the lowering of n_2 and $\chi^{(3)}$ and the modifications in n_2 and $\chi^{(3)}$ value is a very useful parameter for the UV nonlinear optical material, solid state laser (Dong et al. 2018; Zou et al. 2018). However, the Ag diffusion in only Se layer shows increase in susceptibility with decrease in optical bandgap (Naik et al. 2019a) (Fig. 11).

3.4 X-ray photoelectron spectroscopy (XPS)

The changes in the bonding arrangement due to thermal and photo diffusion process can be viewed from the XPS spectra. Being a surface analytic technique, it provides detailed information regarding the atomic movements in the film. The required core level spectra

Fig. 11 Ge 3d core level spectra of GeS, Ag/GeS, illuminated and annealed Ag/GeS thin films



like as Ge $3d$, S $2p$ and Ag $3d$ were measured for the analysis. The Ge $3d$ core level binding energy (BE) shifts towards higher BE values upon Ag deposition and diffusion process on GeS film. The as-prepared Ge $3d$ peak for the GeS film was at 32.02 eV that shifts to 32.65 eV for the irradiated film and 33.45 eV for the annealed film. This was due to the Ag diffusion into the GeS layer which facilitated the formation of Ge–S heteropolar bonds by breaking of Ge–Ge and S–S bonds due to annealing and irradiation. The change in intensity of Ge $3d$ peak indicates the formation of more heteropolar bonds as S has higher electronegativity than that of Ge and Ag (Ge: 2.01, S: 2.58, Ag: 1.93) (Pauling 1960). Similarly, the S $2p$ spectra for the studied films are shown in Fig. 12 in which the peak position for GeS, Ag/GeS, irradiated and annealed Ag/GeS films are located at 163.52, 163.15, 162.61 and 161.53 eV respectively. The shift of 0.54 eV and 1.62 eV for the irradiated and annealed film towards lower BE infers the formation of Ag–S heteropolar bonds as the electronegativity of Ag is less than that of S. Such heteropolar bond formation causes the decrease of the defect states in the gap region thus increasing the optical band gap. The Ag $3d$ peak is absent for the GeS film as seen from Fig. 13. However, the Ag $3d$ peak for the Ag/GeS film was at 359.93 eV that shifted to 1.38 eV and 2.76 eV towards higher BE with irradiation and annealing. This shifting towards higher BE region infers the formation of Ag–S bonds as S has the higher electronegativity than Ag. The intensity of Ag $3d$ peak for the Ag/GeS film decreased for the irradiated and annealed film that shows the diffusion of Ag into GeS layer. Such BE shift of the core level peaks clearly supports the chemical bond rearrangement as a result of thermal annealing and laser irradiation (Naik et al. 2015). However, from the amount of shifting it is clear that Ag diffusion is more in annealed film than the irradiated film. In order to see the oxidation effect, we have plotted the O $1s$ core level spectra in Fig. 14. It is found that the O $1s$ peak which lies at ~531 eV shows nearly equal intensity that infers the same contribution for all the films. Although preparation of the film and characterizations was performed in vacuum condition, the Oxygen content is due to the sample exposure to atmosphere at the time of removal of the prepared film from vacuum coating unit.

The diffusion mechanism of Ag into GeS layer is depicted by a chemical reaction between Ag and GeS chalcogenide induced localized electronic state of Ag. The schematic diagram is shown in Fig. 14. The photo carriers are generated when the photons are being absorbed

Fig. 12 S $2p$ core level spectra of GeS, Ag/GeS, illuminated and annealed Ag/GeS thin films

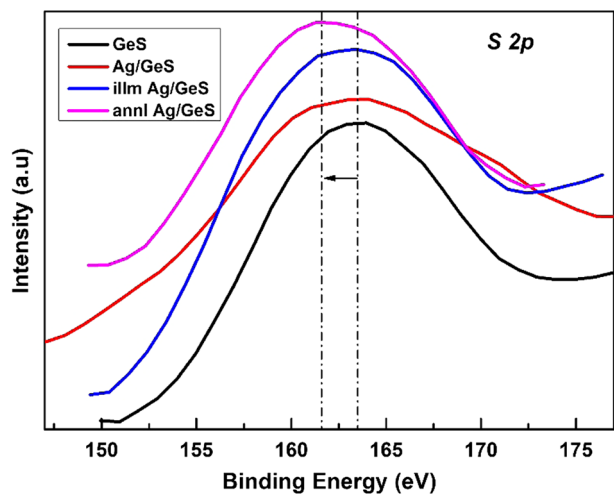


Fig. 13 Ag 3*d* core level spectra of Ag/GeS, illuminated and annealed Ag/GeS thin films

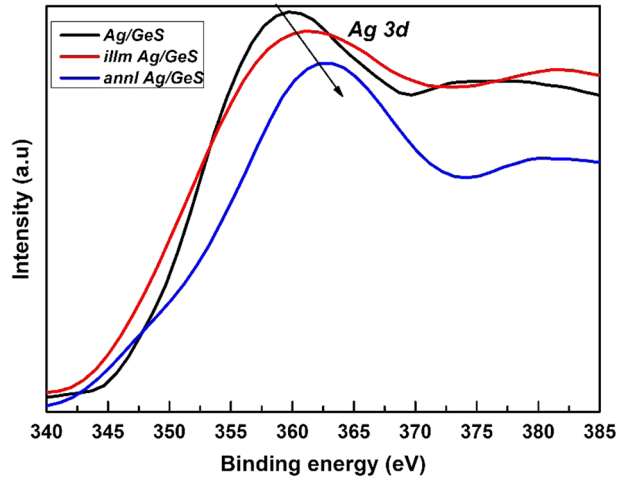
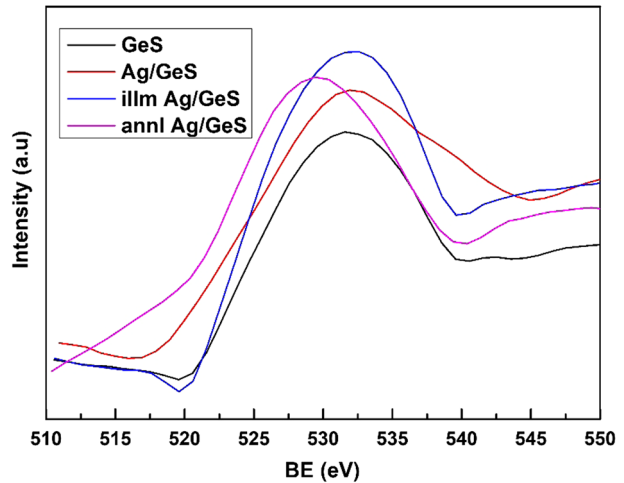


Fig. 14 O1*s* spectra of GeS, Ag/GeS, illuminated and annealed Ag/GeS thin films



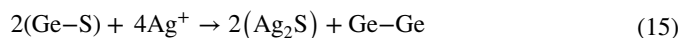
by the chalcogenides at the Ag–GeS interface during laser irradiation (Frumar and Wagner 2003). The electrons are trapped by the active chalcogen (S) atom which shows affinity to Ag⁺ ions. The Ag atoms are ionized as



and the released electron is being captured by the chalcogenide S atoms as



The localized S⁻ states were annihilated by the reaction S⁻ + Ag⁺ → Ag–S that leads to the complete reaction as



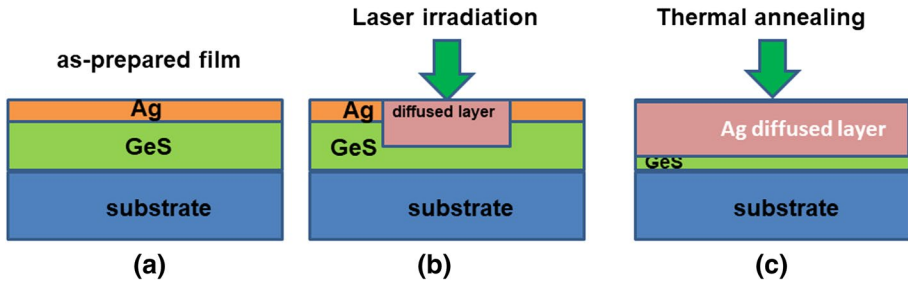
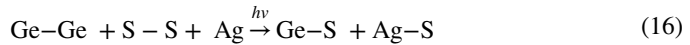


Fig. 15 Schematic diagram of Ag diffusion into GeS layer

The chemical bonds associated with Ge, S bonds interacts with Ag through illumination of laser light by the following process



The formation of Ge-S and Ag-S heteropolar bonds decreases the density of defect states in the gap which increases the optical band gap. Since, Ag is incorporated in the amorphous chalcogenide network that forms small species of Ag₂S and/or fourfold-coordinated Ag atoms decreases the density of the defects (i.e. localized states). This is reflected in the decreasing value of E_u (276 meV) compared to the as deposited Ag/GeS film (282 meV) (Fig. 15).

The decrease in disorder in the photo diffused film is due to the formation of solid solution Ag-S-Ge with laser irradiation as seen from other studies (Malyovanik et al. 2003; Behera and Naik 2016). The thermal annealing of the heterostructure film induces the Ag⁺ ions with more dimension than that of the illumination. The thermal diffusion length of Ag into the GeS layer is approximated as (Dt)^{1/2} where D is the diffusion coefficient and t is the time duration of annealing. The degree of change in thermal diffusion process is found to be more that can be seen from the optical parameters and such type of trend is also observed in other studies (Naik et al. 2019a).

4 Conclusion

In conclusion, the diffusion of Ag into GeS matrix has been studied using thermal annealing and laser irradiation process. The linear and nonlinear optical parameters were influenced by Ag diffusion process. The third order susceptibility and nonlinear refractive index shows a reverse effect with optical band gap. Such changes in the properties makes these materials suitable for fabricating nonlinear optical devices. Thermal and photo induced increase in optical band gap is due to the decrease in density of localised states and disorder. Such tuning of band gap with simple annealing and irradiation helps these materials to be used in designing many optical devices. The increase in transmittance in the film is useful for optical transmitting purpose. The decreasing nature of high frequency dielectric constant ε_∞ tuned by change in free carrier concentration after Ag deposition and diffusion into GeS film is good for optical communication. The magnitude of change in the optical parameters by thermal diffusion process is found to be more than photo diffusion

one as seen from the optical parameters. The chemical bond redistribution by converting homopolar bond to heteropolar bond is being probed by XPS measurement. The linear and nonlinear optical response makes these films a promising candidate for optoelectronic applications.

Acknowledgements The authors thank Board of Research in Nuclear Science (BRNS) for financial support (No. 37(3)/14/02/2016-BRNS/37016) and Department of Physics, Indian Institute of Science (IISc.) for XPS study. The authors are also thankful to NISER, Bhubaneswar for FESEM study.

References

- Abuelwafa, A.A., El-Denglawey, A., Dongol, M., El-Nahass, M.M., Soga, T.: Influence of annealing temperature on structural and optical properties of nano-crystalline platinum octa ethylporphyrin (PtOEP) thin films. *Opt. Mater.* **49**, 271–278 (2015)
- Aparimita, A., Sripan, C., Ganesan, R., Naik, R.: Photo- and thermally induced property change in Ag diffusion into Ag/As₂Se₃ thin films. *Appl. Phys. A* **124**, 267–10 (2018a)
- Aparimita, A., Sripan, C., Ganesan, R., Jena, S., Naik, R.: Influence of thermal annealing on optical and structural properties change in Bi-doped Ge₃₀Se₇₀ thin films. *Phase Trans.* **91**, 862–871 (2018b)
- Attia, A.A., El-Nahass, M.M., El-Bakry, M.Y., Habashy, D.M.: Neural networks modelling for refractive indices of semiconductors. *Opt. Commun.* **287**, 140–144 (2013)
- Atyia, H.E., Hageb, N.A.: Influence of thermal treatment on the optical aspects for Ge₂₀In₃Se₇₅ films. *Optik* **127**, 3888–3894 (2016)
- Barr, T.L., Seal, S.: Nature of the use of adventitious carbon as a binding energy standard. *J. Vac. Sci. Technol. A* **13**, 1239–1246 (1995)
- Behera, M., Naik, R.: Optical properties change in laser-induced Te/As₂Se₃ chalcogenide thin films. *Appl. Phys. A* **122**, 913–9 (2016)
- Behera, M., Behera, S., Naik, R.: Optical band gap tuning by laser induced Bi diffusion into As₂Se₃ film probed by spectroscopic techniques. *RSC Adv.* **7**, 18428–18437 (2017)
- Calvez, L.: Chalcogenide glasses and glass-ceramics: transparent materials in the infrared for dual applications. *C. R. Phys.* **18**, 314–322 (2017)
- Dong, X., Huang, L., Liu, Q., Zeng, H., Lin, Z., Xu, D., Zou, G.: Perfect balance harmony in Ba₂NO₃(OH)₃: a beryllium-free nitrate as a UV nonlinear optical material. *Chem. Commun.* **54**, 5792–5795 (2018)
- Edward, D.P.: Handbook of Optical Constants of Solids. Academic Press Handbook, New York, pp. 547–569 (1985)
- El-Nahass, M.M., El-Den, M.B., El-Mallah, H.M., Abu-Samaha, F.S.: Effect of Pb addition and heat treatment on optical properties of thermally evaporated Ge_{1-x}Se₂Pb_x thin films. *J. Phys. Chem. Solids* **69**, 2652–2659 (2008)
- El-Nahass, M.M., Ali, M.H., Zedan, I.T.: Photo induced changes in linear and nonlinear optical properties of Ge₁₀In₁₀Se₈₀ thin films. *J. Non-Cryst. Solids* **404**, 78–83 (2014)
- Eneva, J., Gushterov, A., Tomerova, B., Mednikarov, B.: The fabrication of microrelief structures in evaporated Ag/a-Ge₃₀S₇₀ layers. *J. Mater. Sci. Mater. Electron.* **10**, 529–531 (1999)
- Fang, J., Wang, J., Cao, X., Man, Y., Liu, C., Cheng, L., Zhang, X., Zhao, H., Zhang, H., Li, J.: Thickness dependence of a giant nonlinear saturable absorption response in GeSb₄Te₇ thin films. *J. Phys. Commun.* **2**, 015009–8 (2018)
- Frumar, M., Wagner, T.: Ag doped chalcogenide glasses and their applications. *Curr. Opin. Solid State Mater. Sci.* **7**, 117–126 (2003)
- Galstyan, A., Messaddeq, S.H., Fortin, V., Skripachev, I., Vallee, R., Galstian, T., Messaddeq, Y.: Tm³⁺ doped Ga–As–S chalcogenide glasses and fibers. *Opt. Mater.* **47**, 518–523 (2015)
- Ganjoo, A., Jain, H.: Millisecond kinetics of photo induced changes in the optical parameters of a-As₂S₃ films. *Phys. Rev. B Condens. Matter Phys.* **74**, 024201–6 (2006)
- Ganjoo, A., Shimakawa, K., Kamiya, H., Davis, E.A., Singh, J.: Percolative growth of photodarkening in amorphous As₂S₃ films. *Phys. Rev. B* **62**, R14601–R14604 (2000)
- Horton, J.H., Hardacre, C., Baddeley, C.J., Moggridge, G.D., Ormerod, R.M., Lambert, R.M.: The effect of photo-oxidation on the sticking and reactivity of Ag on amorphous GeS₂. *J. Phys. Condens. Matter* **8**, 707–718 (1996)

- Kanai, Y., Murakami, Y., Wakaki, M.: Manipulation and observation of Ag photo doping patterns in GeS₂ amorphous films by a dual functional laser scanning fabrication/microscope system. *Appl. Opt.* **49**, 6697–6702 (2010)
- Kawaguchi, T., Maruno, S.: Composition dependence of Ag photo doping into amorphous Ge–S films. *J. Appl. Phys.* **71**, 2195–2201 (1992)
- Kohoutek, T., Mizuno, S., Suzuki, T., Ohishi, Y., Matsumoto, M., Misumi, T.: Third-harmonic generation measurement of nonlinear optical susceptibility⁰ of Ge–Ga–Sb–S chalcogenide glasses proposed for highly nonlinear photonic fibers. *J. Opt. Soc. Am. B* **28**, 298–305 (2011)
- Kolobov, A.V., Elliott, S.R.: Photodoping of amorphous chalcogenides by metals. *Adv. Phys.* **40**, 625–684 (1991)
- Longnos, F., et al.: On the impact of Ag doping on performance and reliability of GeS₂ based conductive bridge memories. *Solid State Electron.* **84**, 155–159 (2013)
- Malyovaniik, M., Ivan, S., Csik, A., Langer, G.A., Beke, D.L., Kokenyesi, S.: Laser-induced optical changes in amorphous multilayers. *J. Appl. Phys.* **93**, 139–142 (2003)
- Mott, N.F., Davis, E.A.: *Electronics Processes in Non-crystalline Materials*, Clarendon, Oxford (1979) p. 428.
- Murakami, Y., Arai, K., Wakaki, M., Shibuya, T., Shintaku, T.: Application of photo-doping phenomenon in amorphous chalcogenide GeS₂ film to optical device. In: *Proceedings SPIE 9359, Optical Components and Materials XII*, 93591N (2015)
- Naik, R., Ganesan, R.: Effect of compositional variations on the optical properties of Sb_xSe_{60-x}S₄₀ thin films. *Thin Solid Films* **579**, 95–102 (2015)
- Naik, R., Ganesan, R., Adarsh, K.V., Sangunni, K.S., Takats, V., Kokenyesi, S.: Insitu pump probe optical absorption studies on Sb/As₂S₃ nanomultilayered film. *J. Non-Cryst. Solids* **355**, 37–42 (2009a)
- Naik, R., Adarsh, K.V., Ganesan, R., Sangunni, K.S., Kokenyesi, S., Deshpande, U., Shripathi, T.: X-ray photoelectron spectroscopic studies on Se/As₂S₃ and Sb/As₂S₃ nanomultilayered film. *J. Non-Cryst. Solids* **355**, 37–42 (2009b)
- Naik, R., Ganesan, R., Sangunni, K.S.: Photo and thermal induced effects on (As₂S₃)_{0.85}Sb_{0.15} amorphous thin films. *J. Non-Cryst. Solids* **357**, 2344–2348 (2011)
- Naik, R., Jena, S., Ganesan, R., Sahoo, N.K.: Photo-induced optical bleaching in Ge₁₂Sb₂₅S₆₃ amorphous chalcogenide thin films: effect of 532 nm laser illumination. *Laser Phys.* **25**, 036001-8 (2015)
- Naik, R., Sahoo, P.P., Sripan, C.: Laser induced Bi diffusion in As₄₀S₆₀ thin films and the optical properties change probed by FTIR and XPS. *Opt. Mater.* **62**, 211–218 (2016)
- Naik, R., Aparimita, A., Sripan, C., Ganesan, R.: Structural, linear and non-linear optical properties of annealed and irradiated Ag/Se heterostructure films for optoelectronic applications. *Optik* **194**, 182894-12 (2019a)
- Naik, R., Behera, A.K., Aparimita, A., Sripan, C., Ganesan, R.: Photo and thermally induced properties change in Bi/Ag/Se trilayer thin film. *Phase Trans.* **92**, 65–78 (2019b)
- Panda, R., Panda, M., Rath, H., Singh, U.P., Naik, R., Mishra, N.C.: Annealing induced AgInSe₂ formation from Ag/In/Ag/In multilayer film for solar cell absorbing layer. *Opt. Mater.* **84**, 618–624 (2018)
- Panda, R., Naik, R., Mishra, N.C.: Thermal annealing induced evolution of AgIn₅Se₈ phase from Ag/In₂Se₃ bilayer thin film. *J. Alloys Compd.* **778**, 819–826 (2019)
- Pauling, L.: *The Nature of the Chemical Bond*, Cornell University Press, Ithaca (1960) p. 664.
- Plesa, C., Turcanu, D., Todirica, C., Nicola, I.: Investigations on infrared chalcogenide glasses used in night vision devices. *Chalcogen Lett.* **12**, 633–638 (2015)
- Pradhan, P., Naik, R., Das, N., Panda, A.K.: Laser induced optical properties change by photo diffusion of Sb into As₂Se₃ chalcogenide thin films. *Opt. Laser Technol.* **96**, 158–165 (2017)
- Rana, A., Singh, B., Sharma, R.: Physical and optical properties of thermally deposited Ge–S–Ga thin films. *J. Non-Cryst. Solids* **482**, 93–99 (2018)
- Rashad, M., Darwish, A.A.A., Farha Al-Said, S.A., Hendi, A.A., Hafiz, M.M.: Formation of Ge₃₅In₈S₅₇ amorphous films for optical applications. *Chin. J. Phys.* **56**, 212–220 (2018)
- Shaaban, E.R., Ismail, Y.A.M., Hassan, H.S.: Compositional dependence of the optical properties of amorphous Se_{80-x}Te₂₀Bi_x thin films using transmittance and reflectance measurements. *J. Non-Cryst. Solids* **376**, 61–67 (2013)
- Shaaban, E.R., Mhamed, M., Ab-el Salem, M.N., Abdel-latif, A.Y., Abdel-Rahim, M.A., Yousuf, E.-S.: Structural, linear and non-linear optical properties of annealed As_{47.5}Se_{47.5}Ag₅ thin films for optoelectronic applications. *Opt. Mater.* **86**, 318–325 (2018)
- Sharma, I., Tripathi, S.K., Barman, P.B.: Thickness-dependent optical properties and nonlinear refractive index of a-Ge–Se–In thin films. *Phase Trans.* **87**, 363–375 (2014)
- Shoulders, T.W., Novak, J., Dussauze, M., Musgraves, J.D., Richardson, K.: Thermal poling behavior and SHG stability in arsenic-germanium sulfide glasses. *Opt. Mater. Exp.* **3**, 700–710 (2013)

- Shpotyuk, O.I., Kasperczyk, J., Kityk, I.V.: Mechanism of reversible photo-induced optical effects in amorphous As_2S_3 . *J. Non-Cryst. Solids* **215**, 218–225 (1997)
- Swanepoel, R.: Determination of the thickness and optical constants of amorphous silicon. *J. Phys. E: Sci. Instrum.* **16**, 1214–1222 (1983)
- Tauc, J.: *Amorphous and Liquid Semiconductors*. Plenum Press, New York (1979) p.159
- Urbach, F.: The long-wavelength edge of photographic sensitivity and of the electronic absorption of solids. *Phys. Rev.* **92**, 1324–1 (1953)
- Valalova, R., Tichy, L., Vlcek, M., Ticha, H.: Far infrared spectra and bonding arrangement in some Ge–Sb–S glasses. *Phys. Status Solidi (a)* **181**, 199–209 (2000)
- Wagner, T., Schroeter, S., Glaser, T., Vlcek, M.: Holographic grating preparation in $Ag/As_{30}S_{70}$ multilayer and bilayer structures. *J. Non-Cryst. Solids* **326&327**, 500–504 (2003)
- Wayne, J.J.: Optical third order mixing in GaAs, Ge, Si, and InAs. *Phys. Rev. B* **178**, 1295–1303 (1969)
- Wemple, S.H., DiDomenico, M.: Behavior of the electronic dielectric constant in covalent and ionic materials. *Phys. Rev. B* **3**, 1338–1351 (1971)
- Xue, B., Nazabal, V., Piasecki, M., Calvez, L., Wojciechowski, A., Rakus, P., Czaja, P., Kityk, I.V.: Photo-induced effects in GeS_2 glass and glass–ceramics stimulated by green and IR Lasers. *Mater. Lett.* **73**, 14–16 (2012)
- Ying, Z., Fen, C., Bin, L., Hui, W., Xiang, S., Xun, D., Hua, N.: Linear and nonlinear optical properties of Sb-doped $GeSe_2$ thin films. *Chin. Phys. B* **24**, 066801–5 (2015)
- Zakery, A., Elliott, S.R.: Optical properties and applications of chalcogenide glasses: a review. *J. Non-Cryst. Solids* **330**, 1–12 (2003)
- Zanatta, A.R., Chambouleyron, I.: Absorption edge, band tails and disorder of amorphous semiconductors. *Phys. Rev. B* **53**, 3833–3836 (1996)
- Zou, G., Lin, Z., Zeng, H., Jo, H., Lim, S., You, T.S., Ok, K.M.: $Cs_3VO(O_2)_2CO_3$: an exceptionally thermostable carbonatoperoxovanadate with an extremely large second-harmonic generation response. *Chem. Sci.* **9**, 8957–8961 (2018)

Publisher's Note Springer Nature remains neutral with regard to jurisdictional claims in published maps and institutional affiliations.